Computed Torque Control for a VSA type Hybrid Shoulder Joint

Sariah Mghames[3], Manuel G. Catalano[2], Antonio Bicchi[1,2] and Giorgio Grioli[2]

I. Introduction

Robotic anthropomorphism has been the study area of many researchers, which led to the conclusion that perceiving similar human features allow robots to be more socially accepted and integrated. It has been stated in [1] that appearance and movements are two sources of inferences that may work in unison or conflict, depending on the degree of integration between the computations implemented, the robot's morphology, the material from which it is made, and the movements patterns scripted. While robot's appearance "sets the context for interaction," the robot's movement "can support action coordination, communicate internal states, and also has its own emotional impact" [2]. One key aspect to the embodiment of functional anthropomorphism in robots is the impedance modulation which can be realized mechanically or via software. One approach to impedance modulation deals with mechanical compliance, used to overcome some limitations of the active impedance control e.g. robustness uncertainty with respect to impacts on portions of the arm that are not equipped with sensors [3]. Mechanical anthropomorphism can be thought as structure and elasto-damping characteristics.

Spherical artificial joints are nowadays gaining an increased interest in robotic applications where anthropomorphism is thought to be of great importance. They present a compact, rigid and highly dynamic structure with a high load capacity. Although their workspace is reduced compared to their serial counterparts, some solutions were presented in the literature as a trade-off between the characteristics of both structures [4], [5]. Applications like teleoperated humanoids and social robots are examples where structural and functional anthropomorphism are of strong interest due to social contact, acceptance and easiness of teleoperation.

The iCub cognitive robot [6] incorporates tendon driven joints to reduce the size of the robot and introduces elasticity that has to be considered in designing control strategies where high forces might be generated. All three motors of iCub shoulder joint are fixed in the shoulder base and not moving with respect to each other resulting in a very light arm structure. In parallel, the iCub wrist is a 2-dof tendon-driven parallel joint with motors integrated in the forearm. The tactile hazardous operations robot (THOR) in [7] is designed with a human-like range of motion hip joint. The lower body of THOR uses linear series elastic actuators (SEAs) to drive each joint.

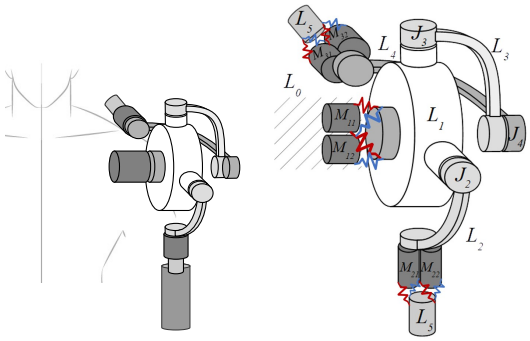

Fig. 1. (a) The generic hybrid shoulder joint configuration [5], (b) The modified variable stiffness actuated hybrid shoulder with nonlinear transmission mechanism

A quasi-anthropomorphic joint structure needs to embed softness in its design. The DLR hand-arm system is based upon the variable stiffness concept which has been recently developed to improve impact robustness and energy efficiency of modern robots [8]. The compliant humanoid COMAN in [9] is actuated by passive compliance actuators [10] based on the series elastic actuation principle. The principle is applied to two out of three serial dofs of the shoulder joint. The genuine design strategy of the elastic iCub shoulder joint presents some complexities from the control point of view, e.g. to obtain the motion of a single joint it is necessary to actuate all the three shoulder motors [11].

The majority of humanoid compliant shoulder joints are either torque controlled in the joint space or controlled by a cartesian active impedance scheme for desired manipulation tasks [12].

In this paper, we present the first prototype of a variable stiffness actuated, hybrid type, robotic shoulder joint. We leverage our work on the anthropomorphic approach presented in our previous work in [5] for humanoids and humans applications. We then formulate the computed torque control scheme for such systems, controlled in fully autonomous scenarios.

As a future work, we will extend the current work with a task learning on one hand, and on the other hand with a human-in-the-loop movement anthropomorphism embodied in feedforward (e.g. in assistive semi-autonomous teleoperation).

[1]Research Center "Enrico Piaggio", Univ. di Pisa, Pisa, Italy
[2]Soft Robotics for Human Cooperation and Rehabilitation, Istituto Italiano di Tecnologia, Genoa, Italy
[3]Lincoln Center for Autonomous Systems, Univ. of Lincoln, United Kingdom
sariahmghames@gmail.com

II. Hybrid joint with Agonist-Antagonist Actuation

To increase anthropomorphism factor in some robotic applications like the remote teleoperation scenario, we combine in this paper the following

- Structural anthropomorphism embodiment in robotic joints: to increase agility, operational workspace and rigidity factors
- Behaviour anthropomorphism of robotic joints through impedance modulation implemented in a passive or active architecture.

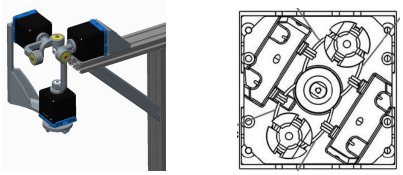

(a) (b)

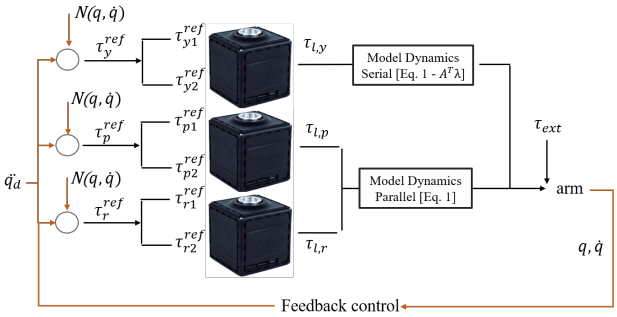

(c)

Fig. 2. (a) A first prototype of the VSA 3-dofs hybrid shoulder joint. (b) Top view of the drive and non-linear elastic mechanism of one dof, [13]. (c) Scheme of the computed torque controller for the VSA 3-dofs hybrid joint.

III. Functionality Testing

The experiment conducted puts in evidence the variation of the robotic joint stiffness in correspondence with that of a user, in a teleoperation scenario. The preset stiffness, input to each dof, is calculated at each time step by first filtering the 8 EMG signals from the MYO armband using a digital filter, then summing and normalizing over them by the maximum sum registered over the time integral.

In fig. 3, the user suddenly stiffens at time t = 38.1s. The root mean square value is calculated for each degree of freedom (dof) and is $[4.8892; 0.79]$ before stiffening and $[4.7136; 0.0901]$ after, for vertical (VFE), horizontal (HFE) flexion-extension dofs, respectively. It is clear that increasing arm stiffness improves the positioning accuracy.

(a) (b)

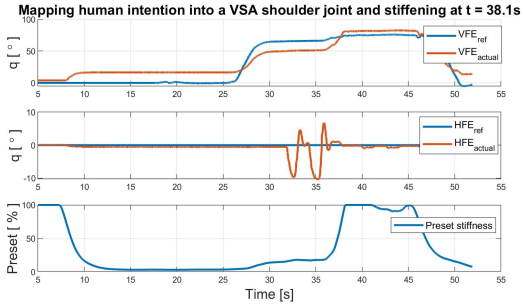

(c)

Fig. 3. Teleoperation with external interaction, (a) case of soft joint, (b) case of stiff arm (c) tracking the vertical and horizontal flexion reference position.

IV. Hybrid Joint Dynamics Control

A. Rigid Hybrid Joint Constrained Dynamics Model

The dynamic model of a closed chain mechanical system (the 2-dof parallel module) can be obtained by virtually cutting the manipulator at one or more of its joints until the complete dynamic model of a tree-like system with several open chains is obtained. Euler-Lagrange formulation is then used for solving the dynamics of each serial chain. Finally, constraint terms obtained by means of the Lagrange Multipliers (λ) are incorporated to include the necessary forces at the splitting points and to ensure a good closure of the kinematic chains.

Based on the Lagrangian $L(q,\dot{q}) = T(q,\dot{q}) - U(q)$, where T the kinetic energy and U the potential energy of the system, the constrained Euler-Lagrange equation of the parallel module is given in the matrix form as

$$\begin{cases} B_c(q)\ddot{q} + C_c(q,\dot{q})\dot{q} + G_c(q) + A_c(q)^T\lambda_c = \tau_c + \tau_{ext} \\ A_c(q)\dot{q} = 0 \quad c = 1,2 \end{cases} \tag{1}$$

where c is the number of legs of the parallel module. The geometric constraints of a parallel manipulator impose that the vector of quasi-position given by $\overline{q} = g(q)$ is 0 such that $\frac{d\overline{q}}{dt} = \frac{\partial g}{\partial q}(q)\dot{q} = A_c(q)\dot{q} = 0$ where $A_c(q)$ is the pfaffian invertible matrix. The geometric constraints are such that the position error between end-effectors $\varepsilon_p = 0$ and orientation error between end-effectors $\varepsilon_o = 0$.
Following the quasi-velocity method to solve the constrained dynamic problem, we have

$$A_c(q)\dot{q} = 0 \rightarrow \dot{q} \in Ker(A_c(q)) \rightarrow \dot{q} = S(q)\,v. \tag{2}$$

Hence, after multiplying by $S(q)^T$, Eq. (1) becomes

$$\dot{v} = (S^T B_c S)^{-1} S^T [\tau_c + \tau_{ext} - (B_c\dot{S} + C_c S)v - G_c)] \tag{3}$$

from which we can retrieve q. $S(q)$ is a base of the Kernel of $A_c(q)$ and v is the vector of quasi-velocity or non-holonomic velocities. The computed torque control law for the hybrid architecture of the VSA multi-dofs joint, is formulated as:

$$\tau_c = \tau_{l,j} = B_c(\ddot{q}_d + K_p e + K_d\dot{q}) + N(q,\dot{q}) \tag{4}$$

where $j \in \{r, p, y\}$ and $N(q, \dot{q}) = C_c(q, \dot{q}) + G_c(q)$. In the particular configuration presented for the shoulder joint, the serial module contributes equally (proportionally to half its inertia) to each chain of the parallel module.

Pfaffian Matrix $\mathbf{A_c(q)}$ Formulation Based on the transformation matrices of both legs in the base frame, i.e T_1^0 and T_2^0, $A_c(q) = \frac{\partial g(q)}{\partial q}$ where $g(q) = [\varepsilon_p(q) \quad \varepsilon_o(q)]^T$, $\varepsilon_p(q) = d_1^0 - d_2^0$ and $\varepsilon_o(q) = R_1^0 - R_2^0$. d_c^0 and R_c^0 define the translation vector and rotation matrix of each leg, respectively.

By reference to [5], we can formulate matrices R_1^0 and R_2^0.

And by reference to the shoulder joint implementation, Denavit-Hartenberg parameters are extracted for each chain, and hence the translation vectors d_1^0 and d_2^0 can be formulated.

Having axis Y_1 of R_1^0 is aligned with Z_2 of R_2^0 and axis X_1 of R_1^0 is aligned with Y_2 of R_2^0, we can write

$$\begin{aligned} -R_1^0(1,2) &= R_2^0(1,3) \\ -R_1^0(2,2) &= R_2^0(2,3) \\ R_1^0(1,1) &= R_2^0(1,2) \end{aligned}$$

we can get $\varepsilon_o(q)$ and hence formulate the 6×5 Pfaffian matrix.

B. Antagonistic VSA Dynamics Model

The soft version of the hybrid shoulder mechanism presented in [5] is illustrated in Fig. 2. The core component of this joint is a variable stiffness actuator with an antagonistic mechanism implemented mechanically in the *qbmove advance*, a derivation of the VSA cube [13]. The antagonistic principle is implemented via two motors connected to the output shaft through a non-linear elastic transmission.

The dynamics of each prime mover of the antagonistic VSA is given by the following,

$$\tau_{j,a}^{ref}(\theta_a) = M_a \ddot{\theta}_a + B_a \dot{\theta}_a + \tau_{sa} \tag{5}$$

for $a = 1, 2$. M_a is the rotor inertia, B_a is a viscous damping factor and τ_{sa} is the nonlinear elastic torque expressed as $K_a \sinh[a_a(q - \theta_a)]$. The VSA output shaft dynamics are then given by

$$\tau_{l,j}(q, \theta_a) = I_l \ddot{q} + B_l \dot{q} + G_l(q) + \tau_{ext} \tag{6}$$

where $\tau_{l,j} = \sum_a \tau_{sa}$. I_l is the link inertia and B_l is the damping factor at the link side. K_a and a_a are parameters of the elastic transmission system identified in [14].

REFERENCES

[1] F. Levillain and E. Zibetti, "Behavioral objects: The rise of the evocative machines," *Journal of Human-Robot Interaction*, vol. 6, no. 1, pp. 4–24, 2017.

[2] G. Hoffman and W. Ju, "Designing robots with movement in mind," *Journal of Human-Robot Interaction*, vol. 3, no. 1, pp. 91–122, 2014.

[3] A. Bicchi and G. Tonietti, "Fast and" soft-arm" tactics [robot arm design]," *IEEE Robotics & Automation Magazine*, vol. 11, no. 2, pp. 22–33, 2004.

[4] R. Reilink, L. C. Visser, D. M. Brouwer, R. Carloni, and S. Stramigioli, "Mechatronic design of the twente humanoid head," *Intelligent service robotics*, vol. 4, no. 2, pp. 107–118, 2011.

[5] S. Mghames, M. G. Catalano, A. Bicchi, and G. Grioli, "A spherical active joint for humanoids and humans," *IEEE Robotics and Automation Letters*, 2019.

[6] G. Metta, G. Sandini, D. Vernon, L. Natale, and F. Nori, "The icub humanoid robot: an open platform for research in embodied cognition," in *Proceedings of the 8th workshop on performance metrics for intelligent systems*, pp. 50–56, ACM, 2008.

[7] B. Lee, C. Knabe, V. Orekhov, and D. Hong, "Design of a human-like range of motion hip joint for humanoid robots," in *ASME 2014 International Design Engineering Technical Conferences and Computers and Information in Engineering Conference*, pp. V05BT08A018–V05BT08A018, American Society of Mechanical Engineers, 2014.

[8] W. Friedl, H. Höppner, F. Petit, and G. Hirzinger, "Wrist and forearm rotation of the dlr hand arm system: Mechanical design, shape analysis and experimental validation," in *2011 IEEE/RSJ International Conference on Intelligent Robots and Systems*, pp. 1836–1842, IEEE, 2011.

[9] N. G. Tsagarakis, S. Morfey, G. M. Cerda, L. Zhibin, and D. G. Caldwell, "Compliant humanoid coman: Optimal joint stiffness tuning for modal frequency control," in *2013 IEEE International Conference on Robotics and Automation*, pp. 673–678, IEEE, 2013.

[10] N. G. Tsagarakis, M. Laffranchi, B. Vanderborght, and D. G. Caldwell, "A compact soft actuator unit for small scale human friendly robots," in *2009 IEEE international conference on robotics and automation*, pp. 4356–4362, IEEE, 2009.

[11] A. Parmiggiani, M. Randazzo, L. Natale, G. Metta, and G. Sandini, "Joint torque sensing for the upper-body of the icub humanoid robot," in *2009 9th IEEE-RAS International Conference on Humanoid Robots*, pp. 15–20, IEEE, 2009.

[12] A. Ajoudani, J. Lee, A. Rocchi, M. Ferrati, E. M. Hoffman, A. Settimi, D. G. Caldwell, A. Bicchi, and N. G. Tsagarakis, "A manipulation framework for compliant humanoid coman: Application to a valve turning task," in *2014 IEEE-RAS International Conference on Humanoid Robots*, pp. 664–670, IEEE, 2014.

[13] M. G. Catalano, G. Grioli, M. Garabini, F. Bonomo, M. Mancini, N. Tsagarakis, and A. Bicchi, "Vsa-cubebot: a modular variable stiffness platform for multiple degrees of freedom robots," in *IEEE International Conference on Robotics and Automation(ICRA 2011)*, pp. 5090–5095, IEEE, 2011.

[14] "qbmove advanced." `https://qbrobotics.com/products/qbmove-advanced/`. Accessed: 2019-03-19.